Available online at www.sciencedirect.com
ScienceDirect
Physics Letters A 372 (2008) 498–509
PHYSICS LETTERS A
www.elsevier.com/locate/pla

Study of intrinsic anchoring in nematic liquid crystals based on modified Gruhn–Hess pair potential

Zhi-Dong Zhang [a], Yan-Jun Zhang [b,c,*]

[a] *Department of Physics, Hebei University of Technology, Tianjin 300130, China*
[b] *Changchun Institute of Optics, Fine Mechanics and Physics, Chinese Academy of Sciences, Changchun 130033, China*
[c] *Graduate School of the Chinese Academy of Sciences, Beijing 100039, China*

Received 15 May 2007; received in revised form 4 July 2007; accepted 24 July 2007

Available online 26 July 2007

Communicated by J. Flouquet

Abstract

A nematic liquid crystal slab composed of N molecular layers is investigated using a simple cubic lattice model, based upon the molecular pair potential which is spatially anisotropic and dependent on elastic constants of liquid crystals. A perfect nematic order is assumed in the theoretical treatment, which means the orientation of the molecular long axis coincides with the director of liquid crystal and the total free energy equals to the total interaction energy. We present a modified Gruhn–Hess model, which is relative to the splay-bend elastic constant K_{13}. Furthermore, we have studied the free nematic interfacial behavior (intrinsic anchoring) by this model in the assumption of the perfect nematic order. We find that the preferred orientation at the free interface and the intrinsic anchoring strength change with the value of modification, and that the director profile can be determined by the competition of the intrinsic anchoring with external forces present in the system. Also we simulate the intrinsic anchoring at different temperatures using Monte Carlo method and the simulation results show that the intrinsic anchoring favors planar alignment and the free interface is more disordered than the bulk.

Keywords: Modified Gruhn–Hess pair potential; Nematic order; Intrinsic anchoring; Director profile; Monte Carlo simulation

1. Introduction

Liquid crystals in restricted geometries are of great interest [1]. In confined nematic liquid crystals with a large surface-to-volume ratio, the aligning effects of the confining surfaces are crucial in determining the equilibrium director configuration. Two major contributions determine the equilibrium director configuration. One is the nematic–substrate interactions and the other is the incomplete anisotropic nematic–nematic interactions in the vicinity of the sample surface. The former is external anchoring and the later is intrinsic anchoring (the anchoring at free nematic interfaces) [2]. The study of anchoring at free nematic interfaces is of importance both in its own right and as a reference for fully confined systems. One of the first experimental investigations of free nematic liquid crystal (NLC) surfaces observed the surface alignment using a light reflection technique and found that p-azoxyanisole (PAA) favors planar ordering [3]. Subsequent work [4] confirmed this result for PAA. Later, another experiment considered the intrinsic anchoring strength and showed that the corresponding extrapolation length is above 100 nm [5]. It is worth stressing that molecular theories are able to model the free interfacial behaviors. A number of simulations of the free interface of nematic liquid crystals have been performed by different potential models so as to investigate how the experimental interfacial phenomena are related to the molecular potentials. For example, intrinsic anchoring has been analyzed by means of a pseudo-

* Corresponding author at: Department of Physics, Hebei University of Technology, Tianjin 300130, China.
E-mail addresses: zhidong_zhang@eyou.com (Z.-D. Zhang), zyj513@hebut.edu.cn (Y.-J. Zhang).

0375-9601/$ – see front matter
doi:10.1016/j.physleta.2007.07.042

molecular model which uses the Maier–Saupe approximation for intermolecular interaction [6]. In addition, some other studies concentrated on the Gay–Berne potential [7] model but chose different parameters [8–10].

In 1996, Gruhn and Hess proposed a spatially anisotropic pair potential depending on the relative position of the particles [11]. It approximately reproduces the elastic free energy density, so that the parameters defining the pair potential can be expressed in terms of the elastic constants. With that, Romano made a Monte Carlo simulation on PAA, for particle centers of mass associated with both a three- [12] and a two-dimensional lattice [13]. In addition, we have dealt with Fréedericksz transition by supposing perfect nematic order in a slab, and obtained a correct expression of the critical field. However, we also found that it cannot induce intrinsic anchoring at free interfaces in perfect nematic order, which is therefore not suitable for studies of intrinsic anchoring [14,15].

In this paper, we are going to investigate a nematic liquid crystal slab composed of N molecular layers (N is finite). In Section 2, a perfect nematic order is assumed in the theoretical treatment. Then based on Gruhn–Hess pair potential model, we evaluate the total energy and find the director profile by minimizing it. In Section 3, using a modified Gruhn–Hess model, we study the free nematic interfacial behaviors and discuss the main results. We give our conclusions in Section 4.

2. Model

2.1. The anisotropic potential model

Let us consider a nematic crystal lattice model. From Ref. [11], the nearest-neighbour pair potential takes the form

$$\Phi_{ik} = \lambda\big[P_2(a_i) + P_2(a_k)\big] + \mu\left(a_i a_k b_{ik} - \frac{1}{9}\right) + \nu P_2(b_{ik}) + \rho\big[P_2(a_i) + P_2(a_k)\big]P_2(b_{ik}), \tag{1}$$

$$\mathbf{r} = \mathbf{p}_i - \mathbf{p}_k, \qquad \mathbf{s} = \mathbf{r}/|\mathbf{r}|, \qquad a_i = \mathbf{u}_i \cdot \mathbf{s}, \qquad a_k = \mathbf{u}_k \cdot \mathbf{s}, \qquad b_{ik} = \mathbf{u}_i \cdot \mathbf{u}_k. \tag{2}$$

Here λ, μ, ν and ρ are the pair-potential parameters which can be expressed in terms of the elastic constants; P_2 is the second-order Legendre polynomial; $\mathbf{p}_i$ and $\mathbf{p}_k$ are three-component dimensionless lattice-point coordinates; $\mathbf{u}_i$ and $\mathbf{u}_k$ denote three-component unit vectors describing the orientations of the two particles; $\mathbf{s}$ is a unit vector pointing from the center of mass of molecule i to the center of mass of molecule k.

2.2. Director profile in a nematic slab with perfect nematic order

Our NLC slab is composed of N molecular layers (N is finite). The surfaces of the slab are assumed to be normal to the z-axis so as to remove the homogeneity in the z direction but not in the x–y plane. We label the molecular layers parallel to the x–y plane by m ($m \in [1, N]$), with $m = 1$ and $m = N$ denoting the two surface layers. In the hypothesis of perfect nematic order, $\mathbf{u}_i$ coincides with the director of the liquid crystals (the statistical average of $\mathbf{u}_i$) and the total free energy coincides with the total intermolecular energy. This is equivalent to assuming that the temperature is zero. Furthermore, we assume the molecular orientation changes only in x–z plane. The director $\mathbf{u}_i$ can be parameterized by the polar angle θ (the angle between the director and the normal of the layer surface)

$$\mathbf{u}_i = (\sin\theta_i, 0, \cos\theta_i). \tag{3}$$

If the molecule i is in the mth layer, $\theta_i = \theta_m$. For the molecule i and its six neighbors, the unit vector $\mathbf{s}$ is given by

$$\mathbf{s}_{i1} = (-1, 0, 0), \qquad \mathbf{s}_{i2} = (1, 0, 0), \qquad \mathbf{s}_{i3} = (0, -1, 0), \qquad \mathbf{s}_{i4} = (0, 1, 0), \qquad \mathbf{s}_{i5} = (0, 0, -1), \qquad \mathbf{s}_{i6} = (0, 0, 1). \tag{4}$$

Substituting Eqs. (3) and (4) into Eqs. (1) and (2), we obtain the total energy of per molecule in the mth layer.

$$\begin{aligned}
\Phi(m) \equiv \Phi(\theta_{m-1}, \theta_m, \theta_{m+1}) &= \sum_{j=1}^{6} \Phi_{ij} \\
&= 2\left\{(\lambda + \rho)\big(3\sin^2\theta_m - 1\big) + \mu\left(\sin^2\theta_m - \frac{1}{9}\right) + \nu\right\} + 2\left(-\frac{1}{9}\mu + \nu - \lambda - \rho\right) \\
&\quad + (1 - \delta_{mN})\left\{\left[\lambda + \frac{3}{2}\rho\cos^2(\theta_m - \theta_{m+1}) - \frac{1}{2}\rho\right]\left[\frac{3}{2}\big(\cos^2\theta_m + \cos^2\theta_{m+1}\big) - 1\right]\right. \\
&\quad \left. + \mu\left[\cos\theta_m\cos\theta_{m+1}\cos(\theta_m - \theta_{m+1}) - \frac{1}{9}\right] + \nu\left[\frac{3}{2}\cos^2(\theta_m - \theta_{m+1}) - \frac{1}{2}\right]\right\} \\
&\quad + (1 - \delta_{m1})\left\{\left[\lambda + \frac{3}{2}\rho\cos^2(\theta_m - \theta_{m-1}) - \frac{1}{2}\rho\right]\left[\frac{3}{2}\big(\cos^2\theta_m + \cos^2\theta_{m-1}\big) - 1\right]\right. \\
&\quad \left. + \mu\left[\cos\theta_m\cos\theta_{m-1}\cos(\theta_m - \theta_{m-1}) - \frac{1}{9}\right] + \nu\left[\frac{3}{2}\cos^2(\theta_m - \theta_{m-1}) - \frac{1}{2}\right]\right\}.
\end{aligned} \tag{5}$$

Here we introduce two factors $(1-\delta_{m1})$ and $(1-\delta_{mN})$, since molecules in the first layer have no lower neighboring molecules and molecules in the Nth layer have no upper neighboring molecules.

If an external magnetic field $\mathbf{H}$ is applied to the NLC molecule, the potential of a NLC molecule induced by magnetic fields is [16]

$$f_M = -\frac{1}{2}\eta_a(\mathbf{H}\cdot\mathbf{u}_i)^2, \tag{6}$$

where $\eta_a = \eta_\parallel - \eta_\perp$ is the magnetic anisotropy of NLC molecule. If the molecule i is in the mth layer, Eq. (6) gives

$$f_M(m) = -\frac{1}{2}\eta_\alpha(H_x\sin\theta_m + H_z\cos\theta_m)^2. \tag{7}$$

Boundary conditions are typically fixed by the interaction with substrates in a nematic slab, or, alternatively, through orienting effects near free nematic interfaces. If there is interaction of weak external anchoring, we assume the interaction between the molecule i (in the interfaces) and the substrate is as follows [17]

$$g_S(\mathbf{u}_i, \boldsymbol{\Pi}) = -\frac{1}{2}\varepsilon_s(\mathbf{u}_i\cdot\boldsymbol{\Pi})^2. \tag{8}$$

Here ε_s is a positive constant and $\boldsymbol{\Pi}$ is the easy orientation. If the polar angles of the two-substrate easy orientation are θ_0 and θ_0' respectively, i.e.,

$$\boldsymbol{\Pi} = (\sin\theta_0, 0, \cos\theta_0), \tag{9a}$$

$$\boldsymbol{\Pi}' = (\sin\theta_0', 0, \cos\theta_0'). \tag{9b}$$

We can obtain by Eq. (9)

$$g_{S1} = -\frac{1}{2}\varepsilon_s\cos^2(\theta_1-\theta_0), \tag{10a}$$

$$g_{SN} = -\frac{1}{2}\varepsilon_s\cos^2(\theta_N-\theta_0'). \tag{10b}$$

The total energy of the sample is obtained by summing up the single molecular energies given by Eqs. (5), (7) and (10) over all the m layers

$$F = \sigma\sum_{m=1}^{N}\left[\frac{1}{2}\Phi(m) + f_M(m)\right] + \sigma(g_{S1}+g_{SN}), \tag{11}$$

where σ is the molecular density per unit surface and $\sigma \propto 1/a^2$.

The total free energy given by Eq. (11) should be minimized with respect to all variables θ_m. It leads to the necessary condition

$$\frac{\partial F}{\partial\theta_m} = 0 \quad (m = 1, 2, \ldots, N). \tag{12}$$

Substituting Eq. (11) into Eq. (12), yields

$$\begin{aligned}
&(3\lambda+3\rho+\mu)\sin 2\theta_m - (1-\delta_{mN})\left\{\frac{3}{2}\rho\sin 2(\theta_m-\theta_{m+1})\left[\frac{3}{2}\left(\cos^2\theta_m+\cos^2\theta_{m+1}\right)-1\right]\right.\\
&\left.+\frac{3}{2}\left[\lambda+\frac{3}{2}\rho\cos^2(\theta_m-\theta_{m+1})-\frac{1}{2}\rho\right]\sin 2\theta_m+\mu\cos\theta_{m+1}\sin(2\theta_m-\theta_{m+1})+\frac{3}{2}\nu\sin 2(\theta_m-\theta_{m+1})\right\}\\
&-(1-\delta_{m1})\left\{\frac{3}{2}\rho\sin 2(\theta_m-\theta_{m-1})\left[\frac{3}{2}\left(\cos^2\theta_m+\cos^2\theta_{m-1}\right)-1\right]\right.\\
&\left.+\frac{3}{2}\left[\lambda+\frac{3}{2}\rho\cos^2(\theta_m-\theta_{m-1})-\frac{1}{2}\rho\right]\sin 2\theta_m+\mu\cos\theta_{m-1}\sin(2\theta_m-\theta_{m-1})+\frac{3}{2}\nu\sin 2(\theta_m-\theta_{m-1})\right\}\\
&-\eta_a(H_x\sin\theta_m+H_z\cos\theta_m)(H_x\cos\theta_m-H_z\sin\theta_m)+\delta_{m1}\left[\frac{1}{2}\varepsilon_s\sin 2(\theta_m-\theta_0)\right]+\delta_{mN}\left[\frac{1}{2}\varepsilon_s\sin 2(\theta_m-\theta_0')\right]=0\\
&\quad(m=1,2,\ldots,N).
\end{aligned} \tag{13}$$

3. The modified Gruhn–Hess pair potential model

3.1. The modification of potential model

By the argument outlined in Ref. [11], the four potential parameters λ, μ, ν, ρ are defined through the following combinations of elastic constants (called Gruhn–Hess pair potential model), including a factor Λ, with dimension of a length:

$$\lambda = \frac{1}{3}\Lambda(2K_{11} - 3K_{22} + K_{33}), \tag{14a}$$

$$\mu = 3\Lambda(K_{22} - K_{11}), \tag{14b}$$

$$\nu = \frac{1}{3}\Lambda(K_{11} - 3K_{22} - K_{33}), \tag{14c}$$

$$\rho = \frac{1}{3}\Lambda(K_{11} - K_{33}). \tag{14d}$$

Let us consider a NLC slab with free interfaces, i.e., there are no external magnetic fields and no external substrate anchoring. One can demonstrate that

$$\theta_{m-1} = \theta_m = \theta_{m+1} = \theta \tag{15}$$

are the solutions of Eq. (13) for $m = 2, 3, \ldots, N-1$. For homogeneousness, the two equations for $m = 1$ and for $m = N$ reduce to

$$(3\lambda + 3\rho + \mu)\sin 2\theta = 0. \tag{16}$$

Substituting Eqs. (15) and (16) into Eq. (11), we find that

$$F = \sigma\left[(N-2)\left(\frac{2}{3}\mu + 3\nu\right) + (3\lambda + 3\rho + \mu)\sin^2\theta + \left(5\nu + \frac{4}{9}\mu\right) - 2(\lambda + \rho)\right]. \tag{17}$$

Eq. (14) gives $3\lambda + 3\rho + \mu = 0$ and the director in the slab is isotropic. So, Gruhn–Hess model does not induce intrinsic anchoring at free interfaces and is not suitable for studies of nematic surface behavior. However, when in a three-dimensional period boundary conditions, upon summing over all interacting pairs, the term $\lambda[P_2(a_i) + P_2(a_k)]$ in the pair potentials cancels out identically [18], i.e., the value of λ does not influence the description of the NLC bulk properties. In addition, as seen from Appendix A, three basic Fréedericksz transitions do lead to Eqs. (14b)–(14d) and do not concern Eq. (14a) [14], i.e., μ, ν and ρ are independent but λ is not. The value of λ in the original model can be given by $3\lambda + 3\rho + \mu = 0$. So we expect a modified λ for a modified model to describe the behavior of nematic interfaces. The potential parameters of modified model are related to the elastic constants as follows

$$\lambda = \frac{1}{3}\Lambda(2K_{11} - 3K_{22} + K_{33} + K_x), \tag{18}$$

K_x is a factor to describe the behavior of nematic interfaces. When $K_x = 0$, it reduces to Eq. (14a) of the original model.

3.2. A slab of free nematic liquid crystal

If not considering the layers of surfaces ($m = 1$ and $m = N$) and taking out the external magnetic fields, we expand Eq. (5) into Taylor series at the point $(\theta_m, \theta_m, \theta_m)$.

$$\begin{aligned}\Phi(m) = {} & \Phi(\theta_m, \theta_m, \theta_m) + \left.\frac{\partial\Phi}{\partial\theta_{m-1}}\right|_{\substack{\theta_{m-1}=\theta_m \\ \theta_{m+1}=\theta_m}}(\theta_{m-1} - \theta_m) + \left.\frac{\partial\Phi}{\partial\theta_{m+1}}\right|_{\substack{\theta_{m-1}=\theta_m \\ \theta_{m+1}=\theta_m}}(\theta_{m+1} - \theta_m) + \frac{1}{2}\left.\frac{\partial^2\Phi}{\partial\theta_{m-1}^2}\right|_{\substack{\theta_{m-1}=\theta_m \\ \theta_{m+1}=\theta_m}}(\theta_{m-1} - \theta_m)^2 \\ & + \frac{1}{2}\left.\frac{\partial^2\Phi}{\partial\theta_{m+1}^2}\right|_{\substack{\theta_{m-1}=\theta_m \\ \theta_{m+1}=\theta_m}}(\theta_{m+1} - \theta_m)^2 + \frac{1}{2}\left.\frac{\partial^2\Phi}{\partial\theta_{m+1}\partial\theta_{m-1}}\right|_{\substack{\theta_{m-1}=\theta_m \\ \theta_{m+1}=\theta_m}}(\theta_{m+1} - \theta_m)(\theta_{m-1} - \theta_m) + \cdots.\end{aligned} \tag{19}$$

For the modified model, considering $(\theta_m - \theta_{m+1})$ and $(\theta_{m-1} - \theta_m)$ is small enough, and neglecting the ranks after the second rank, we find that it can be transformed into a continuous form

$$\Phi(\theta) = -2\Lambda(K_{11} + K_{22} + K_{33}) - \frac{1}{2}\Lambda a^2 K_x\frac{d}{dz}\left(\sin 2\theta\frac{\partial\theta}{\partial z}\right) + 3\Lambda a^2\left(K_{11}\sin^2\theta + K_{33}\cos^2\theta\right)\left(\frac{\partial\theta}{\partial z}\right)^2. \tag{20}$$

In the continuum theory of nematics, the bulk elastic energy densities can be written as [19]

$$\begin{aligned}f = {} & \frac{1}{2}\left[K_{11}[\nabla\cdot\mathbf{n}]^2 + K_{22}\left[\mathbf{n}\cdot(\nabla\times\mathbf{n})\right]^2 + K_{33}\left[\mathbf{n}\times(\nabla\times\mathbf{n})\right]^2\right] + K_{13}\nabla\cdot\left[\mathbf{n}(\nabla\cdot\mathbf{n})\right] \\ & - K_{24}\nabla\cdot\left[\mathbf{n}(\nabla\cdot\mathbf{n}) + \mathbf{n}\times(\nabla\times\mathbf{n})\right],\end{aligned} \tag{21}$$

where K_{24} (saddle-splay) and K_{13} (splay-bend) are the elastic constants. When $\mathbf{n}$ depends just on a single Cartesian coordinate, the K_{24} contribution vanishes identically. When $K_{24} = K_{13} = 0$, it degenerates to the ordinary Frank elastic energy densities [20]

$$f = \frac{1}{2}\big[K_{11}[\nabla \cdot \mathbf{n}]^2 + K_{22}\big[\mathbf{n} \cdot (\nabla \times \mathbf{n})\big]^2 + K_{33}\big[\mathbf{n} \times (\nabla \times \mathbf{n})\big]^2\big]. \tag{22}$$

Let us assume the director of liquid crystal $\mathbf{n}$ changes only in x–z plane. Thus

$$\mathbf{n} = (\sin\theta, 0, \cos\theta). \tag{23}$$

Substituting Eq. (23) into Eq. (21), we can obtain

$$f = \frac{1}{2}\big[K_{11}\sin^2\theta + K_{33}\cos^2\theta\big]\left(\frac{\partial\theta}{\partial z}\right)^2 - \frac{1}{2}K_{13}\frac{d}{dz}\left(\sin 2\theta\frac{\partial\theta}{\partial z}\right). \tag{24}$$

From Eq. (20), we yield

$$\frac{\Phi(\theta)}{6\Lambda a^2} = -\frac{1}{3a^2}(K_{11} + K_{22} + K_{33}) - \frac{1}{12}K_x\frac{d}{dz}\left(\sin 2\theta\frac{\partial\theta}{\partial z}\right) + \frac{1}{2}\big(K_{11}\sin^2\theta + K_{33}\cos^2\theta\big)\left(\frac{\partial\theta}{\partial z}\right)^2. \tag{25}$$

If setting $K_x = 6K_{13}$, we find that $\frac{\Phi(\theta)}{6\Lambda a^2}$ is consistent with the Frank elastic free energy density with surface terms (only less a constant). When $K_x = 0$, it degenerates to the Frank elastic free energy density without surface terms. So, the K_x contribution is equivalent to the K_{13} contribution. So, our modified model is written as

$$\lambda = \frac{1}{3}\Lambda(2K_{11} - 3K_{22} + K_{33} + 6K_{13}), \tag{26a}$$

$$\mu = 3\Lambda(K_{22} - K_{11}), \tag{26b}$$

$$\nu = \frac{1}{3}\Lambda(K_{11} - 3K_{22} - K_{33}), \tag{26c}$$

$$\rho = \frac{1}{3}\Lambda(K_{11} - K_{33}). \tag{26d}$$

Substituting Eq. (26) into Eqs. (16) and (17), we can obtain

$$6\Lambda K_{13}\sin 2\theta = 0, \tag{27}$$

$$F = \Lambda\sigma\left[-\left(N - \frac{1}{3}\right)(K_{11} + K_{22} + K_{33}) + 6K_{13}\sin^2\theta - 4K_{13}\right]. \tag{28}$$

If $K_{13} > 0$, Eq. (27) gives $\theta = 0$ (homeotropic alignment to free surfaces) so that the total energy is lowest. If $K_{13} < 0$, $\theta = \pi/2$ (planer alignment to free surfaces). If K_{13} is zero, the free interfaces cannot produce any orienting effects. The main consequence of the modification occurs in the form of intrinsic anchoring. To characterize this intrinsic anchoring we introduce the intrinsic anchoring strength ε_I. We can see that the form of Eq. (28) looks like Rapini–Papoular anchoring [21]. If we set $\varepsilon_I = 6\sigma\Lambda K_{13}$, we find that the source of intrinsic anchoring can be reduced to a term formally identical to K_{13} term.

3.3. A slab of free nematic liquid crystal in a magnetic field

We continue to consider a slab of free NLC in a magnetic field in order to know more information about intrinsic anchoring. First, let us consider $K_{13} > 0$. From Section 3.2, it favors homeotropic alignment to free surfaces. We assume the angle between the direction of $\mathbf{H}$ and the surface normal is α. When α is small enough (but it is not zero), the direction of the magnetic field is close enough to the homeotropic intrinsic anchoring easy axis. The phenomenological solution for the director profile $\theta(z)$ can also be obtained from the ordinary Frank elastic theory (Eq. (22)) by adding the $w_S = \frac{1}{2}\varepsilon_I\theta^2$ (intrinsic anchoring form as external anchoring) and $f_M = -\frac{1}{2}\chi_a(\mathbf{H}\cdot\mathbf{n})^2$ (the magnetic energy term) and then carrying out the ordinary variational minimization procedure. We get a profile for the symmetric sample as follow

$$\theta(z) = \alpha + A\frac{\cosh(\frac{z-d/2}{\xi})}{\cosh(\frac{d}{2\xi})}, \tag{29}$$

where the parameter A is related to the amplitude of the deformation, d is the sample thickness, and ξ is the characteristic length of this field-induced deformation (it is also called the magnetic coherence length), $\xi = \sqrt{\frac{K_{33}}{H^2\chi_a}}$.

When θ is small enough (since α is small enough), we can obtain from Eqs. (13) and (26),

$$3\Lambda(K_{33} + 2K_{13})\theta_1 - 3\Lambda K_{33}\theta_2 + \eta_a H^2(\theta_1 - \alpha) = 0, \tag{30a}$$

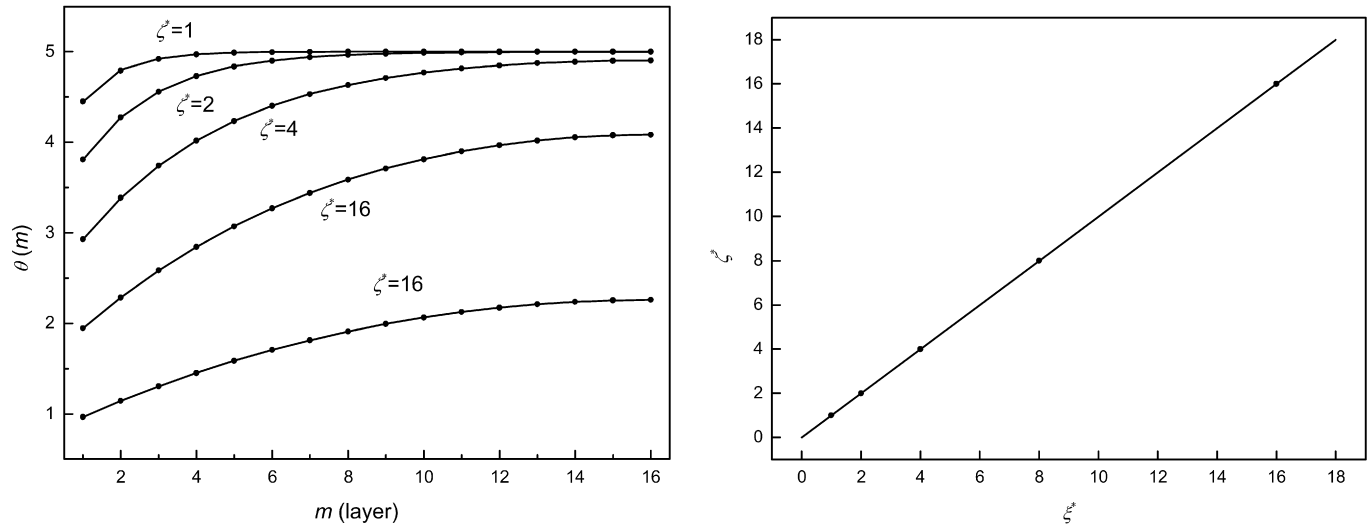

Fig. 1. Magnetic-field-induced distortions for $K_{13}^* = 0.1$ and different values of ς^*; the angle between the field **H** and the surface normal is equal to $\alpha = 5^\circ$. (a) Dots denote calculated director profiles with Eq. (29) and solid lines the director profiles with Eq. (31). The sample thickness is equal to $N = 31$ layers. (b) The dependence ς^* vs ξ^* for the upper case.

$$-3\Lambda K_{33}(\theta_{m-1} - 2\theta_m + \theta_{m+1}) + \eta_a H^2(\theta_m - \alpha) = 0 \quad (m = 2, \ldots, N-1), \tag{30b}$$

$$3\Lambda(K_{33} + 2K_{13})\theta_N - 3\Lambda K_{33}\theta_{N-1} + \eta_a H^2(\theta_N - \alpha) = 0. \tag{30c}$$

We have noted that the K_{13} term disappeared in Eq. (30b). If setting $\chi_a = \eta_a/a^3$ and $K'_{33} = 3\Lambda K_{33}/a$, we find that Eq. (30b) is consistent with the bulk Frank elastic equation, i.e.,

$$-K'_{33}\frac{\theta_{m-1} - 2\theta_m + \theta_{m+1}}{a^2} + \chi'_a H^2(\theta_m - \alpha) = 0 \tag{31}$$

where K'_{33} and χ'_a are corresponding with K_{33} and χ_a in the continuum theory. So we set $\varsigma = \sqrt{\frac{3\Lambda K_{33}/a}{H^2\eta_a/a^3}}$, which is the corresponding magnetic coherence length.

$$\left[(\varsigma/a)^2 + 2(\varsigma/a)^2 K_{13}^*\right]\theta_1 - (\varsigma/a)^2\theta_2 + (\theta_1 - \alpha) = 0, \tag{32a}$$

$$-(\varsigma/a)^2(\theta_{m-1} - 2\theta_m + \theta_{m+1}) + (\theta_m - \alpha) = 0 \quad (m = 2, N-1), \tag{32b}$$

$$\left[(\varsigma/a)^2 + 2(\varsigma/a)^2 K_{13}^*\right]\theta_N - (\varsigma/a)^2\theta_{N-1} + (\theta_N - \alpha) = 0, \tag{32c}$$

where $K_{13}^* = K_{13}/K_{33}$ is dimensionless. Here it is convenient to introduce two-dimensionless parameters $\varsigma^* = \varsigma/a$ and $\xi^* = \xi/a$.

Numeric results are plotted in Figs. 1(a), (b) and (2). In Fig. 1(a), director profiles for various values of the parameter ς^* and $K_{13}^* = 0.1$, i.e., for different field strengths and the same intrinsic anchoring, are shown. The magnetic field **H** determines the orientation of molecules in the bulk far from the surface, while it competes with the intrinsic anchoring close to the surface. The stronger the magnetic field, the smaller the lengths ξ^* and ς^*. The curves of Eq. (29) (solid lines) with only one characteristic length (ξ^*) are in agreement with the profiles calculated from our model (dots). This means that all our profiles can be described by the Frank elastic theory (neglecting the K_{13} contribution), by adding the external-like anchoring contributions. We also obtain that ξ^* is equal to ς^*, plotted in Fig. 3(b).

In Fig. 2, we plotted the director profiles for $\varsigma^* = 8$ and different values of $K_{13}^* = 0.01$, $K_{13}^* = 0.05$, $K_{13}^* = 0.1$, $K_{13}^* = 0.2$. We can find that, for the same field strength, if the intrinsic anchoring strength is stronger, there are the bigger effects to director profiles near the surface.

Certainly, when $K_{13} < 0$, we can obtain similar results. Differently, it favors planner alignment to free surfaces.

3.4. A slab of nematic liquid crystal with external anchoring

There is always real surface anchoring in real nematic cells, which in principle can have an easy axis, different from the one intrinsic anchoring favors. Both external anchoring and intrinsic anchoring determine the equilibrium director configuration. External anchoring is the nematic-substrate interactions, which is strong only for those molecules that lie close to the surface. Since effects of the intrinsic anchoring are also restricted to a thin subsurface layer, it is now more difficult to predict the profile resulting from the competition of both anchorings. If there are the symmetric external anchorings for two substrates, i.e., $\theta_0 = \theta'_0$, one can

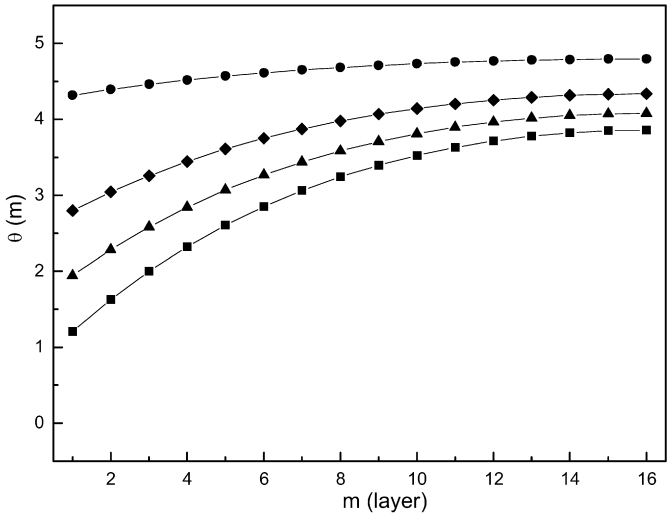

Fig. 2. Magnetic-field-induced distortions for $\varsigma^* = 8$ and different values of $K_{13}^* = 0.01$, $K_{13}^* = 0.05$, $K_{13}^* = 0.1$, $K_{13}^* = 0.2$ (circles, diamonds, triangles, and squares, respectively); the angle between the field **H** and the surface normal is equal to $\alpha = 5^\circ$.

demonstrate that

$$\theta_{m-1} = \theta_m = \theta_{m+1} = \theta \tag{33}$$

is the solution to Eq. (13) (taking out external magnetic fields) for $m = 2, 3, \ldots, N-1$. For homogeneousness, the two equations for $m = 1$ and for $m = N$ reduce to

$$(3\lambda + 3\rho + \mu)\sin 2\theta + \varepsilon_s \sin 2(\theta - \theta_0) = 0. \tag{34}$$

By Eq. (26), $3\lambda + 3\rho + \mu = 6\Lambda K_{13}$. If setting $\tau = (3\lambda + 3\rho + \mu)/\varepsilon_s = 6\Lambda K_{13}/\varepsilon_s = \varepsilon_I/\varepsilon_s$, we can obtain

$$\tan 2\theta = \frac{\sin 2\theta_0}{\cos 2\theta_0 + \tau}. \tag{35}$$

The value of τ determines the director profile. When $\tau = 0$, i.e., there is no intrinsic anchoring, the director profile is equal to the two-substrate easy orientation θ_0. When $\tau \neq 0$, both external anchoring and intrinsic anchoring determine the director profile. The director profile consists in the competition of external anchoring strength ε_s with the intrinsic anchoring strength ε_I.

3.5. Computer simulations of the intrinsic anchoring

From the assumption of perfect nematic order, we have obtained a modified Gruhn–Hess potential model and have studied the free nematic interfacial behavior by this model in the assumption of the perfect nematic order. Furthermore, we compute the behavior of nematic interfaces at nonzero temperatures using the modified Gruhn–Hess model.

Romano has made a Monte Carlo simulation of the bulk for PAA [12]. Since the value of λ is related to K_{13} and it is difficult to search for a reference of the K_{13} for PAA, we choose the elastic constants of 5CB (4-n-pentyl-4'-cyanobiphenyl) at 25 °C [22], i.e.,

$$K_{11} = 5.85 \times 10^{-12}\ \text{N}, \qquad K_{22} = 3.50 \times 10^{-12}\ \text{N}, \qquad K_{33} = 7.80 \times 10^{-12}\ \text{N}. \tag{36}$$

The splay-bend constant [23] is

$$K_{13} = -0.2K_{11}. \tag{37}$$

We calculated coefficients λ, μ, ν, ρ by Eq. (26) and then rescaled by dividing by $|\nu|$; thus the potential model under investigation becomes

$$\Phi_{ik} = \varepsilon\left\{\lambda\big[P_2(a_i) + P_2(a_k)\big] + \mu\left(a_i a_k b_{ik} - \frac{1}{9}\right) + \nu P_2(b_{ik}) + \rho\big[P_2(a_i) + P_2(a_k)\big]P_2(b_{ik})\right\}. \tag{38}$$

The pair potential parameters are

$$\lambda = 0.15904, \qquad \mu = -1.6988, \qquad \nu = -1, \qquad \rho = -0.15663. \tag{39}$$

Anchoring effects usually are characterized within phenomenological approaches by two parameters: the easy axis and the anchoring strength. The nematic-substrate interaction is given by Eq. (8). We define a dimensionless anchoring strength parameter as $w = \varepsilon_s/\varepsilon$.

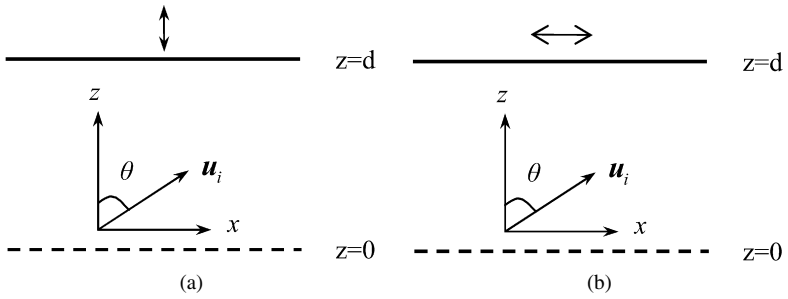

Fig. 3. Two NLC slabs: (a) The top interface is a substrate with strong external hometropic anchoring and the bottom interface is a free interface described with a dashed line. (b) The top interface is a substrate with strong external planar anchoring and the bottom interface is a free interface. $\theta = \theta(z)$ is the usual polar angle which is measured with respect to z-axis.

We choose two NLC slabs in order to study the intrinsic anchoring easy axis and the intrinsic anchoring strength, as shown in Fig. 3(a) and Fig. 3(b). In Fig. 3(a), the top ($z = d$) interface is taken to be a substrate with strong external anchoring ($w = 10$) and the easy axis $\boldsymbol{\Pi} = (0, 0, 1)$. The bottom ($z = 0$) interface where the intrinsic anchoring will be measured is a free interface described with a dashed line. Fig. 3(b) shows that the top ($z = d$) interface is taken to be a substrate with strong external anchoring ($w = 10$) and the easy axis $\boldsymbol{\Pi} = (1, 0, 0)$. The bottom ($z = 0$) interface is also a free interface. Clearly, if the easy axis of the free interface is planar, the first slab (Fig. 3(a)) forms a hybrid cell-like nematic sample and the second slab forms a planar one; if the easy axis of the free interface is homeotropic, the first slab (Fig. 3(a)) forms a homeotropic cell-like nematic sample and the second slab forms a hybrid one.

Simulations are performed on cubic samples and the simulation box size is chosen to be 32^3. We use periodic conditions in the x and y directions, and only consider interactions between nearest neighbors. In numerical calculation, the scaled temperature $T^*(T^* = k_B T/\varepsilon)$ is introduced. We apply the Metropolis algorithm [24] to update the lattice and to find the state of the lowest energy. Instead of comparing different configurations, one (arbitrary) director distribution is taken and the free energy E_p is calculated. Then we select a random point of the configuration altered by a random amount. Furthermore we calculate the energy E_n and the energy difference ΔE between old and new configuration. If ΔE is negative, i.e., the altered director field has a lower energy than the unaltered one, the move is accepted. If ΔE is positive, i.e., the change of the director increases the energy, the move is not immediately discarded but accepted with a probability of $p = e^{-\Delta E/k_B T}$. Thus a liquid crystal system at some temperature T reaches its thermal equilibrium by a large quantity of runs. Our equilibration runs take 10^5 Monte Carlo cycles and production runs take 10^5 cycles.

We have calculated the second rank tensor after the system reaching thermal equilibrium in order to calculate the director profile $\theta(z)$.

$$Q_{\alpha\beta}(z) = \left(3\left\langle u_i^{\alpha} u_i^{\beta}\right\rangle_z - \delta_{\alpha\beta}\right)/2. \tag{40}$$

Here α and β can be x, y or z, and u_i^{α} refers to the α component of the unit vector $\mathbf{u}_i$. Firstly, the average $\langle\cdots\rangle_z$ is performed over all particles for current configuration in the layer centered at z. Then the current second rank ordering tensor is diagonalized. Accordingly, the director is identified by the eigenvector associated with the eigenvalue possessing the largest magnitude and the second-order parameter is equal to the largest magnitude eigenvalue. Lastly, the director and the second-order parameter average over the production Monte Carlo cycles.

As seen from the simulation results for 5CB (Figs. 4 and 5), two slabs form a hybrid cell and a planar one. Moreover, the intrinsic anchoring favors planer alignment. Consider the director profiles $\theta(z)$ and the order parameter $s(z)$ at different temperatures respectively in a hybrid nematic cell. One can readily observe that far enough from the NI transition (the nematic-isotropic (NI) transition of the bulk takes place at $T^*_{\mathrm{NI}} = 1.531 \pm 0.001$) the director profiles approach a linear function and they are insensitive to changing temperature. And the order parameter near the free interface is smaller than the bulk one, i.e., the free interface is more disordered than the bulk. Certainly, we also note that it is greatly different when the NI transition temperature is approached, since the layers near surfaces have reached the isotropic phase. From Fig. 5, the director profiles approach a constant ($\theta(z) = \pi/2$) and the order parameter $s(z)$ near the free interface is smaller than the bulk one.

4. Conclusion

In perfect nematic order, we present a modified Gruhn–Hess model, which is relative to the splay-bend elastic constant K_{13}. Using the modified Gruhn–Hess model, we have studied the incomplete intermolecular interaction due to the presence of a bounding surface. This interaction gives rise to an intrinsic anchoring, which introduces a surface easy axis. The direction of this easy axis and the anchoring strength depend on the value of modification. We showed that the bulk source of anchoring can be reduced to pure surface anchoring, a term formally identical to K_{13} term. In addition, a slab of free nematic liquid crystal in a magnetic field

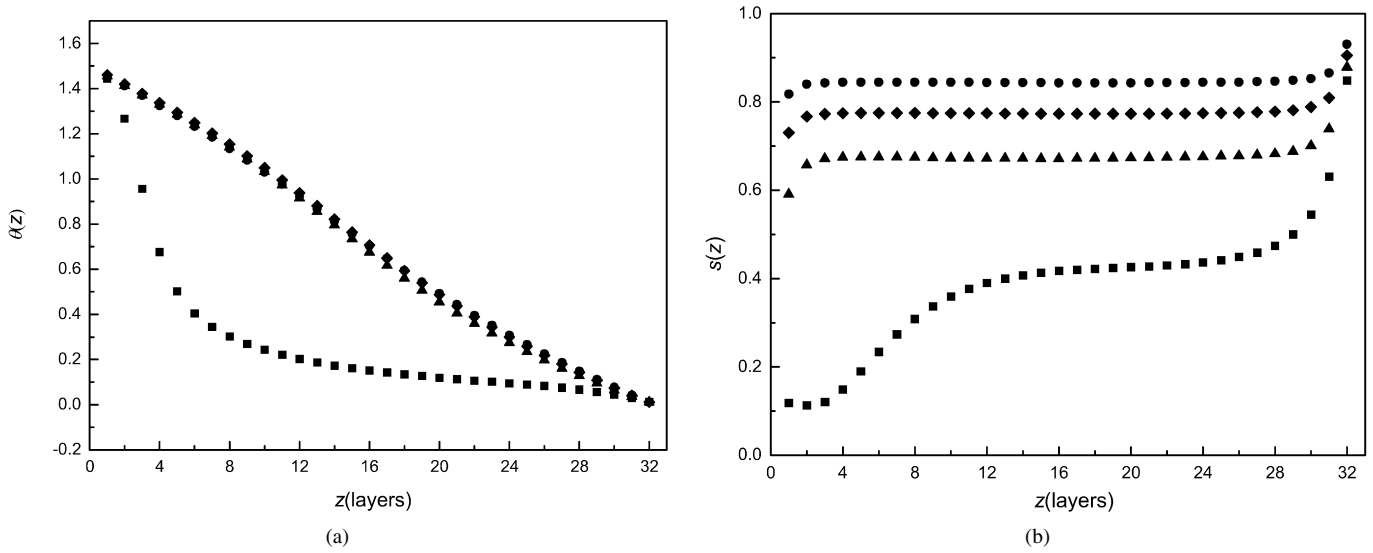

(a) (b)

Fig. 4. A nematic slab with homeotropic anchoring at $z = d$ for 5CB. The scaled temperature: $T^* = 0.75$, $T^* = 1.0$, $T^* = 1.25$ and $T^* = 1.5$ (circles, diamonds, triangles, and squares, respectively) (a) director; (b) order parameter.

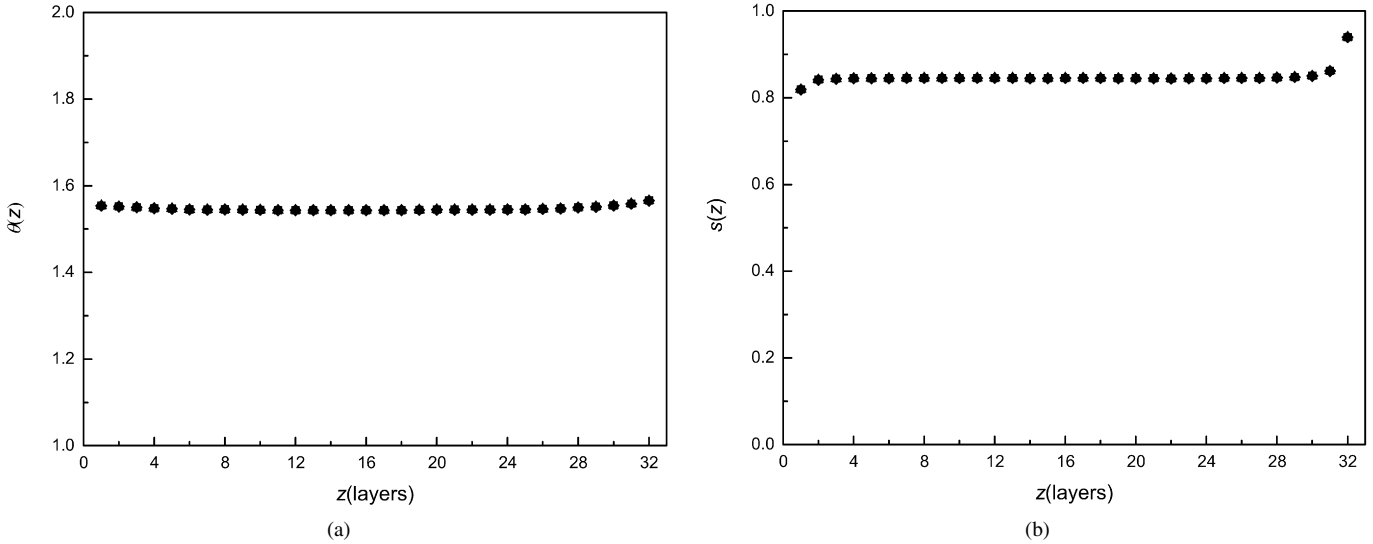

(a) (b)

Fig. 5. A nematic slab with planar anchoring at $z = d$ for 5CB. The scaled temperature: $T^* = 0.75$, $T^* = 1.0$, $T^* = 1.25$ and $T^* = 1.5$ (circles, diamonds, triangles, and squares, respectively) (a) director; (b) order parameter.

and a slab of nematic liquid crystal with external anchoring were well studied. The form of the deformation can be qualitatively explained alone by the competition of the intrinsic anchoring with external forces in the system: the magnetic field, in the former case, and external anchoring, in the latter case. Additionally, the Monte Carlo simulation results at different temperatures for 5CB show that the intrinsic anchoring favors planar alignment, and the free interface is more disordered than the bulk.

Acknowledgements

Project supported by the Natural Science Foundation of Hebei Province, China (103002) and the Key Subject Construction Project of Hebei Provincial University.

Appendix A. Study of distortions in NLC slabs based upon spatially anisotropic pair potential

Distortions of NLC slabs are studied based upon Eqs. (1) and (2). Assuming the perfect nematic order, we investigate three kinds of the basic Fréedericksz transition.

A.1. The homeotropic-to-planar alignment transition

The NLC slab is composed of N molecular layers. The surfaces of the slab are assumed to be normal to the z-axis so as to remove the homogeneity in the z direction but not in the x–y plane. The molecular layers parallel to the x–y plane are labeled by m, with $m = 1$ and $m = N$ denoting the two surface layers. We assume the molecular orientation changes only in x–z plane. We still apply an external magnetic field $\mathbf{H}$ to the NLC molecule. As the Section 2, we can yield balance equations

$$\begin{aligned}
&(3\lambda + 3\rho + \mu)\sin 2\theta_m - (1-\delta_{mN})\left\{\frac{3}{2}\rho\sin 2(\theta_m - \theta_{m+1})\left[\frac{3}{2}\left(\cos^2\theta_m + \cos^2\theta_{m+1}\right) - 1\right]\right.\\
&\left.+\frac{3}{2}\left[\lambda + \frac{3}{2}\rho\cos^2(\theta_m - \theta_{m+1}) - \frac{1}{2}\rho\right]\sin 2\theta_m + \mu\cos\theta_{m+1}\sin(2\theta_m - \theta_{m+1}) + \frac{3}{2}\nu\sin 2(\theta_m - \theta_{m+1})\right\}\\
&-(1-\delta_{m1})\varepsilon\left\{\frac{3}{2}\rho\sin 2(\theta_m - \theta_{m-1})\left[\frac{3}{2}\left(\cos^2\theta_m + \cos^2\theta_{m-1}\right) - 1\right]\right.\\
&\left.+\frac{3}{2}\left[\lambda + \frac{3}{2}\rho\cos^2(\theta_m - \theta_{m-1}) - \frac{1}{2}\rho\right]\sin 2\theta_m + \mu\cos\theta_{m-1}\sin(2\theta_m - \theta_{m-1}) + \frac{3}{2}\nu\sin 2(\theta_m - \theta_{m-1})\right\}\\
&-\eta_a(H_x\sin\theta_m + H_z\cos\theta_m)(H_x\cos\theta_m - H_z\sin\theta_m) = 0 \quad (m = 1, 2, \ldots, N).
\end{aligned} \tag{A.1}$$

The two interfaces of the slab are taken to be substrates, with infinitely strong homeotropic anchoring, i.e., there are equations $\theta_1 = 0$ and $\theta_N = 0$. So Eq. (A.1) is degenerated to $N-2$ equations. Supposing the external magnetic field $\mathbf{H}$ which is applied to the NLC medium is parallel to x-axis (i.e., $H_x = H$, $H_z = 0$) and θ_m is small enough near the threshold magnetic fields, we can reduce Eq. (A.1) to

$$-(6\rho + 3\nu + \mu)(\theta_{m-1} - 2\theta_m + \theta_{m+1}) + \eta_a H^2\theta_m = 0. \tag{A.2}$$

If two sides of Eq. (A.2) are divided by a^3 (a is the lattice constant), we can obtain

$$\frac{-(6\rho + 3\nu + \mu)}{a}\frac{\theta_{m-1} - 2\theta_m + \theta_{m+1}}{a^2} + \frac{\eta_a}{a^3}H^2\theta_m = 0. \tag{A.3}$$

Furthermore, one notes that $(\theta_{m-1} - 2\theta_m + \theta_{m+1})/a^2$ is the difference of $d^2\theta/dz^2$ so that Eq. (A.3) changes to continuous equation.

$$\frac{-(6\rho + 3\nu + \mu)}{a}\frac{d^2\theta}{dz^2} + \frac{\eta_a}{a^3}H^2\theta = 0. \tag{A.4}$$

If setting $\chi_a = \frac{\eta_a}{a^3}$ and $K_{33} = \frac{-(6\rho+3\nu+\mu)}{a}$, we can obtain an equation corresponding with continuous theory. By the same procedure as continuous theory [25], Eq. (A.4) can give the threshold magnetic fields

$$H_C^{(3)} = \frac{\pi}{d}\sqrt{\frac{K_{33}}{\chi_a}}, \tag{A.5}$$

where d is the thickness of NLC slab, i.e., the thickness of NLC cell. We also note χ_a is the magnetic anisotropy of NLC medium if the perfect nematic order is assumed.

A.2. The planar-to-homeotropic alignment transition

We choose two substrates of the slab with infinitely strong planer anchoring which favors planer alignment, i.e., the polar angles of $m = 1$ and $m = N$ satisfy $\theta_1 = \pi/2$ and $\theta_N = \pi/2$. Eq. (A.1) can be degenerated to $n-2$ equations as above. Further, we assume the external magnetic field $\mathbf{H}$ is parallel to z-axis (i.e., $H_x = 0$, $H_z = H$). We can set $\theta_m = \frac{\pi}{2} - \alpha_m$ in order to yield the threshold magnetic fields of Fréedericksz transition by linear analysis. If α_m is small enough, Eq. (A.1) gives

$$(3\rho - 3\nu - \mu)(\alpha_{m-1} - 2\alpha_m + \alpha_{m+1}) + \eta_a H^2\alpha_m = 0. \tag{A.6}$$

According to the same analyses as above, we can yield equations as follows

$$\frac{(3\rho - 3\nu - \mu)}{a}\frac{\alpha_{m-1} - 2\alpha_m + \alpha_{m+1}}{a^2} + \frac{\eta_a}{a^3}H^2\alpha_m = 0, \tag{A.7}$$

$$\frac{(3\rho - 3\nu - \mu)}{a}\frac{d^2\alpha}{dz^2} + \frac{\eta_a}{a^3}H^2\alpha = 0, \tag{A.8}$$

$$H_C^{(1)} = \frac{\pi}{d}\sqrt{\frac{K_{11}}{\chi_a}}, \tag{A.9}$$

where $\chi_a = \eta_a/a^3$, $K_{11} = \frac{3\rho-3\nu-\mu}{a}$.

A.3. The simple twisted transition

We suppose the molecular layer is parallel to the x–y plane as above discussion. But we assume that the direction of molecules changes in x–y plane and that the angle between molecular long axis and x-axis is ϕ. When the molecule i is in the mth layers, $\mathbf{u}_i = (\cos\phi_m, \sin\phi_m, 0)$. The magnetic field is in x–y plane, i.e., $\mathbf{H} = (H_x, H_y, 0)$. By the same procedure as yielding Eq. (A.1), we can obtain

$$-\frac{3}{2}(\nu-\rho)\big\{(1-\delta_{mN})\sin 2(\phi_m-\phi_{m+1}) + (1-\delta_{m1})\sin 2(\phi_m-\phi_{m-1})\big\} - \eta_a(H_x\cos\phi_m + H_y\sin\phi_m)(-H_x\sin\phi_m + H_y\cos\phi_m) = 0 \quad (m = 1, 2, \ldots, N). \tag{A.10}$$

In order to study Fréedericksz transition of twist deformation, we impose the infinitely strong anchoring in x-axis, i.e., $\phi_1 = \phi_N = 0$. The external magnetic fields are parallel to y-axis, i.e., $H_x = 0$, $H_y = H$. Assuming ϕ_m is small enough, we yield

$$-3(\nu-\rho)(\phi_{m-1} - 2\phi_m + \phi_{m+1}) + \eta_a H^2\phi_m = 0. \tag{A.11}$$

As above, we give the equations

$$\frac{-3(\nu-\rho)}{a}\frac{\phi_{m-1} - 2\phi_m + \phi_{m+1}}{a^2} + \frac{\eta_a}{a^3}H^2\phi_m = 0, \tag{A.12}$$

$$\frac{-3(\nu-\rho)}{a}\frac{d^2\phi}{dz^2} + \frac{\eta_a}{a^3}H^2\phi = 0, \tag{A.13}$$

$$H_C^{(2)} = \frac{\pi}{d}\sqrt{\frac{K_{22}}{\chi_a}}. \tag{A.14}$$

Here

$$\chi_a = \frac{\eta_a}{a^3}, \qquad K_{22} = \frac{-3(\nu-\rho)}{a}.$$

A.4. The relations of the potential parameters and the elastic constants

By the relations of the potential parameters and the elastic constants, i.e., $K_{11} = \frac{3\rho-3\nu-\mu}{a}$, $K_{22} = \frac{-3(\nu-\rho)}{a}$, and $K_{33} = \frac{-(6\rho+3\nu+\mu)}{a}$, we can obtain the potential parameters denoted by the elastic constants

$$\mu = 3\Lambda(K_{22} - K_{11}), \tag{A.15a}$$

$$\nu = \frac{1}{3}\Lambda(K_{11} - 3K_{22} - K_{33}), \tag{A.15b}$$

$$\rho = \frac{1}{3}\Lambda(K_{11} - K_{33}). \tag{A.15c}$$

Here $\Lambda = \frac{a}{3}$, which has the dimensions of length. This is consistent with Eqs. (14b), (14c) and (14d) of the Gruhn–Hess model. From above, we cannot obtain the corresponding relation of λ. However, from Ref. [18], the term $\lambda[P_2((a_i)) + P_2(a_k)]$ in the pair potentials cancels out identically when in three-dimensional periodic boundary conditions, i.e., the value of λ does not influence the description of the NLC bulk properties. So we can introduce a modification of λ to describe the behavior of interfaces.

References

[1] G.P. Crawford, S. Žumer (Eds.), Liquid Crystals in Complex Geometries: Formed by Polymer and Porous Networks, Taylor and Francis, London, 1996.
[2] N.V. Priezjev, G. Skačej, R.A. Pelcovits, S. Žumer, Phys. Rev. E 68 (2003) 041709.
[3] M.A. Bouchiat, D. Langevin-Cruchin, Phys. Lett. 34A (1971) 331.
[4] P. Chiarelli, S. Faetti, L. Fronzoni, J. Phys. (Paris) 44 (1983) 1061.
[5] L.M. Blinov, A.Yu. Kabayenkov, A.A. Sonin, Liq. Cryst. 5 (1989) 654.
[6] L.R. Evangelista, S. Ponti, Phys. Lett. A 197 (1995) 55.
[7] J.G. Gay, B.J. Berne, J. Chem. Phys. 74 (1981) 3316.
[8] E. Martin del Rio, E. de Miguel, Phys. Rev. E 55 (1997) 2916.
[9] A.P.J. Emerson, S. Faetti, C. Zannoni, Chem. Phys. Lett. 271 (1997) 241.
[10] S.J. Mills, C.M. Care, M.P. Neal, D.J. Cleaver, Phys. Rev. E 58 (1998) 3284.
[11] T. Gruhn, S. Hess, Z. Naturforsch. A 51 (1996) 1.
[12] S. Romano, Int. J. Mod. Phys. B 12 (1998) 2305.
[13] S. Romano, Phys. Lett. A 302 (2002) 203.
[14] Z.-D. Zhang, Y.-J. Zhang, Acta Phys. Sin. 53 (2004) 2670 (in Chinese).
[15] Y. Zhang, Z. Zhang, Mol. Phys. 105 (2007) 85.

[16] Z.-D. Zhang, D.X. Zhang, Y.B. Sun, Chin. Phys. Lett. 17 (2000) 749.
[17] Z.-D. Zhang, H. Yu, L. Li, Chin. Phys. 10 (2001) 645.
[18] A. Kilian, Liq. Cryst. 14 (1993) 1189.
[19] J. Nehring, A. Saupe, J. Chem. Phys. 54 (1971) 337.
[20] F.C. Frank, Discuss. Faraday Soc. 25 (1958) 19.
[21] A. Rapini, M. Papoular, J. Phys. (Paris) Colloq. 30 (1969) 4.
[22] H.A. Van Spran, H.G. Koopman, J. Appl. Phys. 64 (1988) 4873.
[23] O.D. Lavrentovich, V.M. Pergamenshchik, Phys. Rev. Lett. 73 (1994) 979.
[24] N. Metropolis, A.W. Rosenbluth, M.N. Rosenbluth, et al., J. Chem. Phys. 21 (1953) 1087.
[25] R. Barberi, G. Barbero, in: I.C. Khoo, F. Simoni (Eds.), Physics of Liquid Crystalline Materials, Gorden and Breach Science Publishers, Philadelphia, 1991, p. 215.